Research Article

Basant E.F. ElSaied, Amany M. Diab, Ahmed A. Tayel*, Mousa A. Alghuthaymi, and Shaaban H. Moussa

Potent antibacterial action of phycosynthesized selenium nanoparticles using *Spirulina platensis* extract

https://doi.org/10.1515/gps-2021-0005
received September 15, 2020; accepted November 23, 2020

Abstract: Selenium nanoparticles (SeNPs) are reinforced safe forms of the essential micronutrient selenium (Se) which take a lead in countless biotechnological and biomedical applications. The phycosynthesis of SeNPs was successfully investigated using cell-free extract of the microalgae, *Spirulina platensis*. The phycosynthesized *S. platensis*-SeNPs (*Sp*SeNPs) were characterized using several characterization techniques such as UV-Visible, transmission electron microscopy, Fourier transform infrared spectroscopy, X-ray diffraction, and energy dispersive X-ray. They were effectually achieved using different concentration from sodium selenite (Na_2SeO_3) (1, 5, and 10 mM) to give size means of 12.64, 8.61, and 5.93 nm, respectively, with spherical shapes and highly negative zeta potentialities. The infrared analyses revealed the involvement of many phycochemials in *Sp*SeNPs production. The antibacterial properties of *Sp*SeNPs were confirmed, qualitatively and quantitatively, against foodborne microorganisms (*Staphylococcus aureus* and *Salmonella typhimurium*); the antibacterial activity was correlated and increased with SeNPs' size diminution. The scanning micrographs of *S. typhimurium* cells treated with *Sp*SeNPs indicated the severe action of nanoparticles to destroy bacterial cells in time-dependent manners. The innovative facile phycosynthesis of SeNPs using *S. platensis* is recommended to generate effectual bioactive agents to control hazardous bacterial species.

Keywords: antimicrobial, green synthesis, microalgae extract, *Spirulina platensis*, selenium nanoparticles

1 Introduction

Multidrug-resistant bacteria (MDRB) are well acknowledged to be one of the most vital recent public health problems. The World Health Organization (WHO) identifies antimicrobial resistance (AMR) as "a threat for the effective prevention and treatment of infections" [1]. In this way, growing rates of MDRB have an impact on all responses to global-leading antibiotics such as methicillins, penicillins, and cephalosporins, which in turn cause the development of life-threatening diseases including sepsis, pneumonia, meningitis, and bacteremia [2]. Clinical effectiveness of the emerging drugs is vulnerable leading to even higher rates of MDRB, thus creating a serious predicament that prompted WHO to create an action plan in 2015 [3]. MDRB are showing AMR by drug uptake limitation, drug sites inactivation, and drug efflux [4]. According to Centers for Disease Control and Prevention, more than 2.8 million MDR infections occur in the USA each year, and more than 35,000 people die as a result [5]. Furthermore, WHO stated that if efficient drugs are not provided, the death caused by MDR infections may increase globally to ~10 million by 2050 [6].

Metallic nanoparticles (NPs) have a high potential to confront these predicaments and have been extensively exploited in different biomedical applications such as

* **Corresponding author: Ahmed A. Tayel,** Department of Fish Processing and Biotechnology, Faculty of Aquatic and Fisheries Sciences, Kafrelsheikh University, El-Geish St., 33516, Kafrelsheikh, Egypt, e-mail: tayel_ahmad@yahoo.com, ahmed_tayel@fsh.kfs.edu.eg, tel: +20-10-0196-9909
Basant E.F. ElSaied: Department of Fish Processing and Biotechnology, Faculty of Aquatic and Fisheries Sciences, Kafrelsheikh University, El-Geish St., 33516, Kafrelsheikh, Egypt
Amany M. Diab: Department of Aquaculture, Faculty of Aquatic and Fisheries Sciences, Kafrelsheikh University, El-Geish St., 33516, Kafrelsheikh, Egypt
Mousa A. Alghuthaymi: Department of Biology, College of Science and Humanitarian Studies, Shaqra University, Shaqra, Saudi Arabia
Shaaban H. Moussa: Department of Biology, College of Science and Humanitarian Studies, Shaqra University, Shaqra, Saudi Arabia; Department of Microbial Biotechnology, Genetic Engineering and Biotechnology Research Institute, University of Sadat City, Sadat City, Egypt

antibacterial, antioxidant, and anticoagulant agents [7–14]. Among them, selenium NPs (SeNPs) attracted wide attention because of their exceptional physicochemical properties including biocompatibility, chemical stability, and minimum toxicity [15]. Selenium (Se) is a trace mineral, which is crucial for human health maintenance, with around 40–300 mg as daily regular dietary supplement for adults [16], and its deficiency is known to be related to more than 40 human diseases [17]. The human body degrades SeNPs naturally; the remains of SeNPs act as the Se nutritional source and are nontoxic to the human body [18]. SeNPs have been used as antibacterial agent [19], drug delivery [20], and cancer treatment [21].

Commonly, NPs are formed by chemical or physical approaches. The weaknesses of physical methods include high energy need, low production yield of nanomaterials, and high cost [22]. Likewise, chemical methods are ecologically harmful because of hazardous chemicals involvement [23]. Therefore, biosynthesis is an alternative eco-friendly, easy, and economical method that exploits living creatures such as actinomycetes, algae, bacteria, viruses, fungi, yeast, and metabolites of animals for NPs production. Algae are known as "bio-nanofactories", because both the live/dead biomasses and their extracts were exploited for the phycosynthesis of metallic NPs [24]. In microalgae, the phycosynthesis has been mediated by a plurality of compounds such as amines, amides, alkaloids, terpenoids, phenolics, proteins, and pigments, existing in the crude extracts, which helps in metals reduction and stabilization [25]. To apply this notion, *Spirulina* spp. and its protein-rich extract have been used to synthesize silver NPs [26], gold NPs [27], palladium NPs [28], and titanium dioxide NPs [29]. SeNPs have been biologically synthesized by different bacteria like *Alcaligenes* sp. [30] and plants like leaf extracts of *Diospyros montana* [31].

Therefore, the plan of this research is to apply *Spirulina platensis* extract to phycosynthesize SeNPs (*Sp*SeNPs), to characterize their physiognomies, and to evaluate their antibacterial property against Gram positive and Gram negative foodborne pathogens.

2 Materials and methods

All used materials/reagents were certified analytical grades; Na_2SeO_3 (≥90.0%), ethanol, Sterilized MilliQ Water (MQW), INT 95% (*p*-iodonitrotetrazolium violet), Nutrient broth (NB), and Nutrient agar (NA) were attained from Sigma-Aldrich (St. Louis, MO, USA).

2.1 Phycosynthesis of *Sp*SeNPs

2.1.1 Collection of algal material and preparation of *S. platensis* extract

Dry powder of blue–green microalgae, *S. platensis*, was attained from the Research Algal Farm, Kafrelsheikh University, Egypt. Exactly, 5.0 g of *S. platensis* dried powder was extracted in 50 mL distilled water for 20 min at 80°C. The pasty extract was vacuum filtered and centrifuged (SIGMA, 2-16 KL Germany) at 6,430× *g* for 10 min [32]. The resulting extract was vacuum evaporated at 42°C, and then dried powder was used in further experiments.

2.1.2 *Sp*SeNPs phycosynthesis

MQW was applied for experiments solution preparation. According to Gunti et al. [17], three glass vials containing 10 mL of 1, 5, and 10 mM of Na_2SeO_3 (Sigma-Aldrich) solutions were kept on magnetic stirrer for 30 min to study the effect of Na_2SeO_3 concentration on size and zeta potential of *Sp*SeNPs. Drop-wise addition of freshly prepared *S. platensis* extract solution (2 mL, 1.0% concentration, w/v) was made in each vial. Mixtures were kept under stirrer for 72 h in dark conditions at 25 ± 2°C until the color of sodium selenite solution changed to orange-red, indicating the formation of phycosynthesized *Sp*SeNPs. The pH value was measured for each vial (AD1200, pH meter, Adwaa, Romania).

2.2 Characterization of phycosynthesized *Sp*SeNPs

2.2.1 Surface plasmon resonance (SPR) characteristic

The UV-Visible spectrum of *Sp*SeNPs solution was recorded using a spectrophotometer (model UV-2450, Shimadzu, Japan). The absorbance was measured in the range 200–800 nm.

2.2.2 Fourier transform infrared spectroscopy (FTIR) analysis

Briefly, *Sp*SeNPs solution was dried and ground into a homogeneous powder, and spectra were achieved at

450–4,000 cm^{-1} wave numbers against potassium bromide (KBr) using the spectrophotometer (JASCO spectrometer 4100, Japan). The peaks obtained were plotted as transmittance (%) in *X* axis and wave number (cm^{-1}) in *Y* axis.

2.2.3 Zeta potential (ζ)

The surface charges of *Sp*SeNPs were determined by their zeta potential (Zeta plus, Brookhaven, USA). For sample preparation, 25 µL of *Sp*SeNPs samples was diluted 10 times with water and sonicated for 15 min at 20 Hz. Then mixture was filtered with filter (0.22 µm) and used for zeta potential measurement. The dilution of *Sp*SeNPs was performed to avoid aggregation of NPs. Measurements were obtained in the range of −200 to +200 mV.

2.2.4 Transmission electron microscopy (TEM) imaging

The morphology and size of the phycosynthesized *Sp*SeNPs were characterized using TEM (JEOL, JEM-2100, Japan) operating at an accelerating voltage of 200 kV. The reaction solution was diluted with deionized water and sonicated (Branson-Sonifier 250, USA) for 10 min. The sonicated sample was drop coated on carbon-coated copper grids and vacuum dried for 30 min, and the electron micrographs were taken.

2.2.5 X-ray diffraction (XRD) analysis

XRD measurements were made for *Sp*SeNPs using X-ray diffractometer (XRD-6000, Shimadzu, Japan) with Cu-k_α radiation (λ = 1.5412 Å) at 40 KV and 30 mA in the 2θ range of 10–80° for analysis of purity.

2.2.6 Energy dispersive X-ray (EDX) analysis

The elemental analysis of *Sp*SeNPs was performed by EDX spectroscopy (JSM-IT100, JOEL, Japan).

2.3 Antibacterial potentiality evaluation

The antibacterial potentialities of *S. platensis* extract and *Sp*SeNPs were evaluated, qualitatively and quantitatively, against the challenged bacterial strains. *Salmonella typhimurium* (ATCC 14028) and *Staphylococcus aureus* (ATCC 25923) bacterial strains were used as challenged models. The cultures were propagated and examined in NB and NA media at 37 ± 1°C.

2.3.1 Qualitative assay: Inhibition zone (IZ)

The qualitative assay (using disc diffusion method) was mostly applied in dark to exclude the potential light effect on NPs activity. Bacterial cultures (24 h old) were spread onto NA plates, and then sterile discs (from Whatman No.1 filter paper, 6 mm in diameter) were loaded with 30 µL of *S. platensis* extract or *Sp*SeNPs solutions (each with 100 µg/mL concentration) and positioned on the surfaces of the inoculants. After incubation (for 24 h at 37°C), the appeared IZ diameters were measured, and their triplicates mean was calculated. Clear zone of 25–40 mm, 15–25 mm, 10–15 mm, and <10 mm in diameter was classified as very strong inhibition, strong inhibition, moderate inhibition, and weak inhibition [33]. Ampicillin was used as a standard antibiotic disc for the comparative antibacterial analysis.

2.3.2 Quantitative assay: minimum inhibitory concentration (MIC)

The described microdilution technique [34] was used to determine the MICs of *S. platensis* extract and *Sp*SeNPs against examined foodborne bacteria. In 96-well microplates, the bacterial cultures (~2 × 10^7 CFU/mL) were challenged with serial concentrations from examined agents (in the range of 1–200 µg/mL), then microplates were incubated as mentioned above, and the viability of cells was assessed using chromogenic indicator *p*-iodonitrotetrazolium violet aqueous solution (4% w/v), which produces red-formazan color by active biological cells. Portions from wells containing inhibited cells were plated onto fresh NA plates and incubated to confirm the inhibitory action. The MIC was quantified as the least concentration that prevented bacterial growth in microplates and on NA plates.

2.3.3 Scanning electron microscopy (SEM) imaging

The SEM imaging was used to detect morphological alterations in *S. typhimurium* cells, after exposure to *Sp*SeNPs, for potential elucidation of NPs action mode. The SEM (Hitachi S-500, Tokyo, Japan) bacterial imaging

was conducted using standardized protocol [35]. Grown bacterial cells in NB for 24 h were treated with *Sp*SeNPs (100 µg/mL) for 0 (control), 6, and 12 h at 37°C, then bacterial cells were collected with centrifugation (4,500× *g* for 30 min), washed with saline buffer, re-centrifuged, and subjected to SEM preparation. Dehydrated samples were mounted onto SEM stubs and coated using gold/palladium, and then micrographs were captured.

2.4 Statistical analysis

Triplicated trials were performed and their mean values and standard deviation (SD) were calculated (using Microsoft Excel 2010). Statistical significance calculation at $p \leq 0.05$ was determined using one-way ANOVA using MedCalc software V. 18.2.1 (MedCalc, Mariakerke, Belgium).

3 Results and discussion

3.1 Phycosynthesis of *Sp*SeNPs

Initially, Na_2SeO_3 solution was colorless. After addition of *S. platensis* cell-free extract, the reaction mixture possessed a pale green color. After 24 h, the color of the mixture turned into brownish-orange indicating initial reaction of sodium selenite with the extract. Gradually, the reaction mixture turned into orange-red color which was an indication for *Sp*SeNPs formation (Figure 1). These observations were similar to those stated recently [36].

The cell-free extract was added to Na_2SeO_3 solution; after 72 h, the color changes from green to orange-red color indicating the reduction of SeO_3^{2-} into red Se^0, and it is suggested that the color change was because of the excitation of the SPR. Because of SPR, the reaction mixture color changed from green (before phycosynthesis) to orange-red (after phycosynthesis). Those findings are similar to the results of Faramarzi et al. [37]. They also reported that by SeNPs formation using *Saccharomyces cerevisiae* yeast, the mixture color converted from pale yellow to dark orange. Algal extracts consist of carbohydrates, proteins, minerals, oil, fats, and polyunsaturated fatty acids in addition to bioactive molecules like antioxidants (polyphenols, tocopherols), and pigments like carotenoids (carotene, xanthophyll), chlorophylls, and phycobilins (phycocyanin, phycoerythrin) [38]. From available reports, these potentially active compounds have been elucidated as reducing and stabilizing agents [24]. It has been

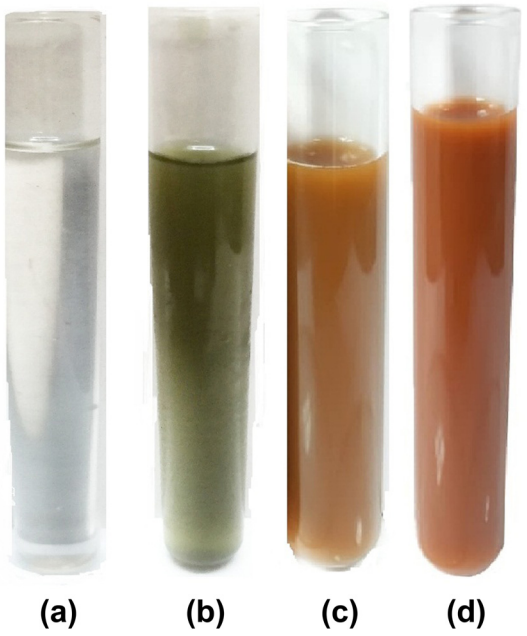

Figure 1: Visual observations of Na_2SeO_3 (10 mM) solution (a), *Spirulina platensis* cell-free extract (b), initial reaction of Na_2SeO_3 with the extract (c), and *Spirulina*-selenium nanoparticles (*Sp*SeNPs) after synthesis completion (d).

recorded that *Spirulina* extracts contain potent biomolecules such as small peptides, proteins, alcohols, phenols, phycocyanins, esters, and amines, which can act as reducing and stabilizing agents [39]. These biomolecules, definitely, facilitated and participated in the reaction with SeO_3^{2-} to produce *Sp*SeNPs, which is insoluble in water [18].

3.2 Characterization of phycosynthesized *Sp*SeNPs

3.2.1 SPR characteristic

UV-Visible analysis was used to confirm the formation of *Sp*SeNPs. *Sp*SeNPs formation was visually recognized by color changing of the reaction mixture from colorless into orange-red. The absorption peak at 270 nm because of the SPR of *Sp*SeNPs is shown in Figure 2. According to literature, because of SPR of SeNPs, they had a broad absorption peak (λ_{max}) at UV-Visible wavelength ranged from 270 to 400 nm [37,40].

3.2.2 FTIR analysis

According to Figure 3a, the cell-free extract of *S. platensis* showed strong transmission peaks at 3,441, 2,848, 2,930,

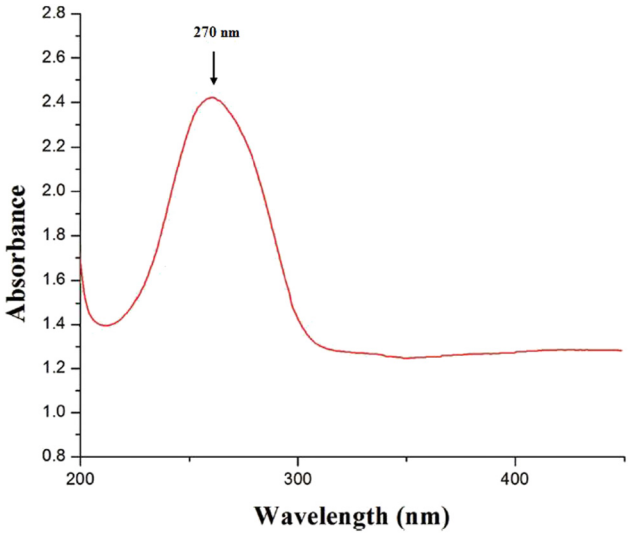

Figure 2: UV-Visible spectrum of *Sp*SeNPs.

1,630, 1,541, 1,407, 1,450, 1,081, and 1,242 cm^{-1}. The peak at 3,441 was referred as O–H stretching vibration because of the presence of alcohol and phenol groups. The appeared peaks ot 2,848 and 2,930 cm^{-1} are due to the C–H stretching vibration of alkenes. The sharp peak at 1,650 and 1,541 cm^{-1} was responsible for C=O stretching and N–O asymmetric stretching vibration of nitro compounds, respectively. The bands at around 1,408 and 1,450 cm^{-1} are attributed to C–C stretch and methylene

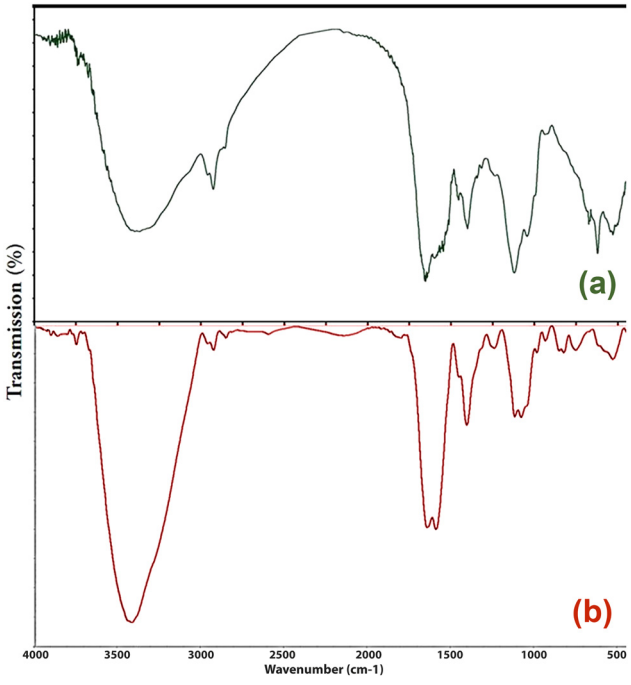

Figure 3: FTIR spectra of *Spirulina* extract (a) and *Sp*SeNPs (b).

scissoring vibrations present in the proteins, respectively. Moreover, the C–N stretching vibration of aliphatic amines and the N–H stretching of the primary and secondary amines could be responsible for peaks at 1,081 and 1,242 cm^{-1}, respectively. Comparable results were formerly reported regarding these functional biochemical bonds [27].

According to Figure 3b, phycosynthesized *Sp*SeNPs showed that the broad intense peak at 3,441 cm^{-1} of cell-free extract of *S. platensis* was shifted to 3,421 cm^{-1} of *Sp*SeNPs, which suggested that Se has interacted with the hydroxyl group from aqueous cell-free extract of *S. platensis* through hydrogen bonding and facilitated phycosynthesis of *Sp*SeNPs [17]. Likewise, the peak 1,450 cm^{-1}, which corresponds to methylene scissoring vibrations present in the proteins of cell-free extract, has disappeared in the phycosynthesized *Sp*SeNPs, which imply that methylene scissoring vibrations present in the proteins have enabled the synthesis of *Sp*SeNPs [52]. Similarly, the sharp peaks at 1,630 and 1,541 cm^{-1} in the *S. platensis* extract, which were responsible for C=O stretching and N–O asymmetric stretching vibration of nitro compounds, were both shifted to higher frequencies 1,650 and 1,592 cm^{-1} in phycosynthesized *Sp*SeNPs, respectively, which shows the interaction of carbonyl C=O stretch and nitro compounds of cell-free extract of *S. platensis* with Se. Two strong absorption peaks of C–N stretching vibration of aliphatic amines and the N–H stretching of the primary and secondary amines at 1,081 and 1,242 cm^{-1}, respectively, are indicative of protein character of phycosynthesized *Sp*SeNPs that may be responsible for reduction and stabilization [31]. From the FTIR, it can be indicated that the bio-organics like proteins, esters, amino acids, and carbonyl β-unsaturated ketone amides phycochemicals from *S. platensis* extract served as a strong capping and reducing agents on *Sp*SeNPs [39].

3.2.3 Zeta potential (ζ)

ζ is not an actual measurement of the individual molecular surface charge; rather, it is a measurement of the electric double layer produced by the surrounding ions in solution. Typically, NPs with ζ values greater than +30 mV or less than −30 mV exhibit high degrees of stability because of the inter-particle electrostatic repulsion [48]. The photosynthesized NPs *Sp*SeNPs were confirmed to be negatively charged, which indicates higher stability of the NPs without forming aggregates at pH range of 8.5 ± 0.5 for the three reactions. Particularly, increasing the sodium selenite concentrations increased the zeta potential values of the phycosynthesized *Sp*SeNPs (Table 1). These

results indicate that increasing the precursor concentration leads to increase in ζ values, which will eventually cause colloidal instability and irreversible aggregation [49]. Zeta values are also known to be influenced by several parameters including pH [50] and extract concentration [51]. The negative charge ζ value could be measured because of the reducing agents of the *Spirulina* extract (e.g., phycocyanin), which reveals the existence of electrostatic forces with the phycosynthesized *Sp*SeNPs [47]. The best nanocomposite (*Sp*SeNPs-A) resulted from the evaluated Na_2SeO_3 concentrations (Table 1), with the least particle size, was subjected for further experiments and characterization.

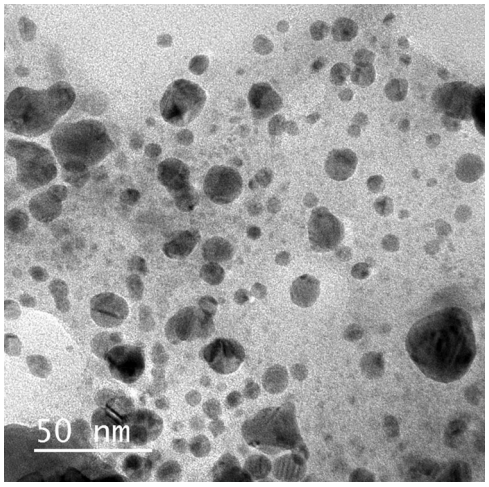

Figure 4: TEM micrographs of phycosynthesized *Sp*SeNPs.

3.2.4 TEM imaging

In Figure 4, the NPs (*Sp*SeNPs-A) are spherical, uniformly distributed, measured size from 2.8 to 38.9 nm, and approximately crystalline in nature. The stoichiometric ratio of the extract and metal precursor is a factor that affects the size and shape of phycosynthesized NPs. Therefore, the concentrations of sodium selenite precursor mainly affected the size of NPs [41].

Particularly, increasing the sodium selenite concentrations increased the particle size range of the phycosynthesized *Sp*SeNPs (Table 1). This indicates that increasing the precursor concentration leads to increase in particle size. These results were coordinated with those mentioned by Kumar et al. [42]. Similarly, the particle sizes of AgNPs and AuNPs were found to be larger at higher metal ion concentrations [43], and that also lately confirmed [44–46]. Particle size is also known to be influenced by other parameters such as extract concentration. The sizes and shapes of SeNPs were dependent on the extract used, which may be attributed to the reduction potential of the extract. It also depends on the capping ability of the phycochemicals that exist in the cell-free extract of *S. platensis* [47].

3.2.5 XRD analysis

The XRD pattern revealed the formation of crystalline phycosynthesized *Sp*SeNPs. The XRD spectrum showed strong diffraction peaks at 23.22° (100), 29.52° (101), 41.14° (110), 43.60° (102), 45.50° (111), 51.48° (201), 55.50° (202), 61.40° (112), 64.88° (210), and 71.40° (113), respectively (Figure 5). All the diffraction peaks in the 2θ range correspond to the hexagonal structure of Se with lattice constants $a = 4.357$ Å and $c = 4.945$ Å and have good agreement with the standard JCPDS data (JCPDS No. 06-0362). However, some noise background was noticed, which may be attributable to the existence of bioactive compounds present in the *S. platensis* extract.

3.2.6 EDX analysis

Figure 6 shows the EDX of *Sp*SeNPs which reveals the presence of 55.21%, 20.43%, 19.26%, and 5.19% for C, N, O, and Se, respectively. This indicates the phycosynthesis of *Sp*SeNPs which contain other elements because of the presence of bioactive compounds of the *S. platensis* extract. However, Zhang et al. [53] attributed the increased proportion of C to the copper mesh of the electron microscope, which is a typical carbon support film.

3.3 Antibacterial potentiality evaluation

The antibacterial potentiality of the cell-free extract of *S. platensis* (S) and phycosynthesized *Sp*SeNPs (*Sp*SeNPs-A,

Table 1: Characteristic attributes of the phycosynthesized *Sp*SeNPs using different concentrations from Na_2SeO_3

Nanoparticles	Na_2SeO_3 concentration (mM)	Size range (nm)	Median diameter (nm)	Mean diameter (nm)	Z-potential (mV)
*Sp*SeNPs-A	1	2.8–38.9	9.7	5.93	−37.4
*Sp*SeNPs-B	5	5.7–41.1	11.8	8.61	−36.1
*Sp*SeNPs-C	10	8.2–50.8	14.2	12.64	−34.6

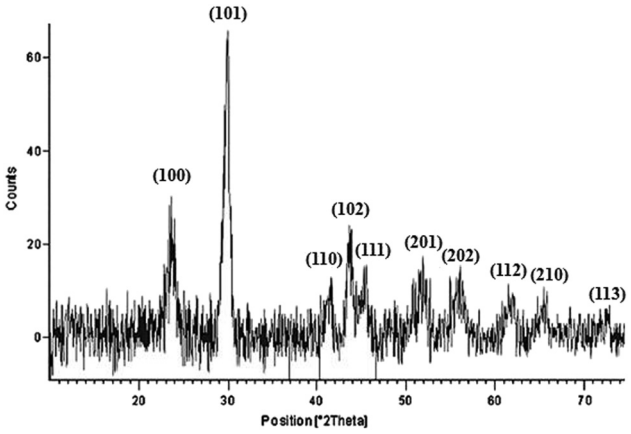

Figure 5: XRD spectrum of *Sp*SeNPs.

*Sp*SeNPs-B, and *Sp*SeNPs-C) was investigated toward *S. aureus* (Gram positive) and *S. typhimurium* (Gram negative) strains.

3.3.1 Qualitative assay: IZ

The results indicate that the smaller the mean diameter of NPs, the wider the diameter of IZ. Therefore, the highest antibacterial potentiality of *Sp*SeNPs against the two strains (15.3 mm for *S. typhimurium* and 18.7 mm for *S. aureus*) was for *Sp*SeNPs-A which possess the smallest particle mean diameter (Table 2). There is a robust relationship between the size of the NPs and their biological activity [45,54]. In the aspect of size-dependent antibacterial activity, the smaller-sized NPs have extra surface area that interact with the bacterial cell membrane, and thus have the greatest interaction with bacteria. This interaction may lead to the increase in penetrability of the outer membrane, which leads to the entry of NPs into cells and affects the cellular response [55]. The effect of many sizes of Ag NPs on the antibacterial activity against *E. coli* was studied [56]; the order of antibacterial activity of Ag NPs of diverse diameter was 10 > 20 > 70 nm.

Another example confirmed that smallest NPs exhibit the best antibacterial action against *E. coli* and *S. aureus* [57]; because of their size, they can simply reach the nuclear content of bacteria when compared to 29 and 89 nm. In addition, a 100 µg of SeNPs produced from cow urine extract showed a weak IZ of 8.4 ± 5.7 mm for *S. aureus* [58], whereas a 100 µL of SeNPs produced from *Allium sativum* extract showed strong IZ of 27 mm for *S. typhimurium* [59]. The IZs of *Sp*SeNPs of the current study were wider than those reported by Fardsadegh and Jafarizadeh-Malmiri [60]. They used *Aloe vera* leaf extract to synthesize SeNPs which showed IZ of 10 mm against *S. aureus*. Moreover, the use of such low concentration of Na_2SeO_3 was found to have no antibacterial effect which is

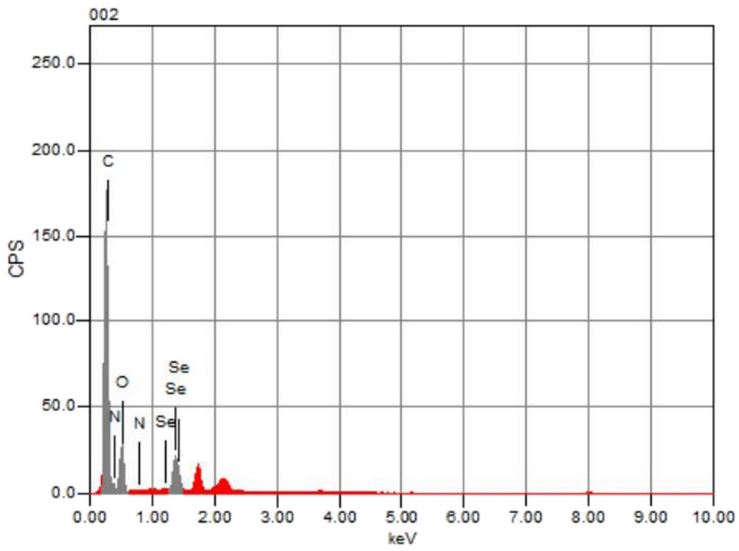

Acquisition Condition
Instrument : IT100LA
Volt : 15.00 kV
Current : ---
Process Time : T3
Live time : 50.00 sec.
Real Time : 50.60 sec.
DeadTime : 1.00 %
Count Rate : 2230.00 CPS

Formula	mass%	Atom%	Sigma	Net	K ratio	Line
C	55.12	62.72	0.03	189504	0.0338535	K
N*	20.43	19.93	0.11	11623	0.0176764	K
O	19.26	16.45	0.08	34474	0.0214272	K
Se	5.19	0.90	0.05	42826	0.0241338	L
Total	100.00	100.00				

Figure 6: EDX analysis of *Sp*SeNPs.

Table 2: Antimicrobial potentialities of *Sp*SeNPs phycosynthesized by *S. platensis* extract

Examined agents	Antibacterial activity**			
	S. typhimurium		*S. aureus*	
	IZ (mm)*	MIC (µg/mL)	IZ (mm)	MIC (µg/mL)
Ampicillin	8.2 ± 1.5	≥100	12.4 ± 0.3	≥100
(*S*) extract	ND	≥100	7.2 ± 0.4^{a}	≥100
*Sp*SeNPs-A	15.3 ± 1.4$^{b@}$	22.5	18.7 ± 1.6^{c+}	17.5
*Sp*SeNPs-B	13.1 ± 1.1$^{a\&}$	27.5	14.4 ± 1.3$^{b\&}$	25
*Sp*SeNPs-C	12.7 ± 0.9^{a+}	30	13.9 ± 1.1^{b+}	27.5

*Inhibition zones present means of triplicates ± standard deviation, including diameter of disc assay (6 mm) that loaded with 100 µg from nanoparticles, standard drug, and extract.· **Dissimilar superscript symbols (in the same row) and letters (in the same column) indicate significant difference (at $p < 0.05$).

similar to the findings in previous reports [61], whether (S) alone showed a weak IZ toward *S. aureus* and no IZ toward *S. typhimurium*; this can be referred to the interaction of lipids in the extract with cellular membrane of Gram positives, and impermeability of the lipopolysaccharide's barrier and absence of teichoic acids within the cell wall of Gram negatives [62]. The standard drug (ampicillin) possessed a moderate IZ for *S. aureus* (12.4 mm) and a weak IZ toward *S. typhimurium* (8.2 mm) in comparison to the phycosynthesized *Sp*SeNPs.

3.3.2 Quantitative assay: MIC

After challenging the bacteria with 1–200 µg/mL serial concentrations of *Sp*SeNPs, the results indicate that the smaller the particle size of *Sp*SeNPs, the smaller the MIC value (Table 2). This shows that *Sp*SeNPs-A, which possessed the smallest particle size, can inhibit bacteria at a lower MIC (22.5 µg/mL for *S. typhimurium* and 17.5 µg/mL for *S. aureus*), whereas *Sp*SeNPs-C which possess the largest particle size can inhibit bacteria at a higher concentration for the two strains (30.0 µg/mL for *S. typhimurium* and 27.5 µg/mL for *S. aureus*). These findings were in line with those recently mentioned [63]. In addition, it has been reported that the higher the SeNP concentration, the higher the inhibition effect on the various bacterial strains [64]. SeNPs produced from propolis extract inhibited *S. aureus* and *S. typhimurium* at MIC of 250 µg and 1,000 µg, respectively [36].

3.3.3 SEM imaging

Compared to the control (Figure 7a), SEM micrographs manifested that the treated bacterial cell walls of *S. typhimurium* had been deformed after 6 h of exposure to *Sp*SeNPs-A (100 µg/mL); many cells were lysed and their internal constituents started to leak (Figure 7b). After 12 h of exposure, most of the treated *S. typhimurium* cells were lysed, and the few residual intact cells were observed in a pond of leaked internal constituents (Figure 7c).

Numerous reports suppose that Se may attach to the cell membrane surface disturbing penetrability and respiratory role of the cell. Probably, SeNPs not only interact with the surface of membranes but can also penetrate inside the bacteria [36,65].

The cell membrane damage of *S. typhimurium* was found to be because of increasing oxidative enzyme activities after treatment with *Sp*SeNPs-A and therefore increasing generation of reactive oxygen species [66–68].

4 Conclusion

This research showed successful phycosynthesis of *Sp*SeNPs with *S. platensis* cell-free extract via a simple, cost-effective, eco-friendly nanobiotechnological method. Phycosynthesized *Sp*SeNPs were characterized using several characterization techniques such as UV-Visible, TEM, FTIR, XRD, and EDX. The phycosynthesis of *Sp*SeNPs was achieved using different concentration from Na_2SeO_3 (1, 5, and 10 mM) to give *Sp*SeNPs size means of 12.64, 8.61, and 5.93 nm, respectively, with spherical shapes and highly negative zeta potentialities. These *Sp*SeNPs manifested potent antibacterial potentiality against pathogenic $Gram^-$ and $Gram^+$ bacterial strains compared to a common commercial antibiotic because of the combined active phycochemicals. The scanning micrographs of treated *S. typhimurium* cells indicated that antibacterial

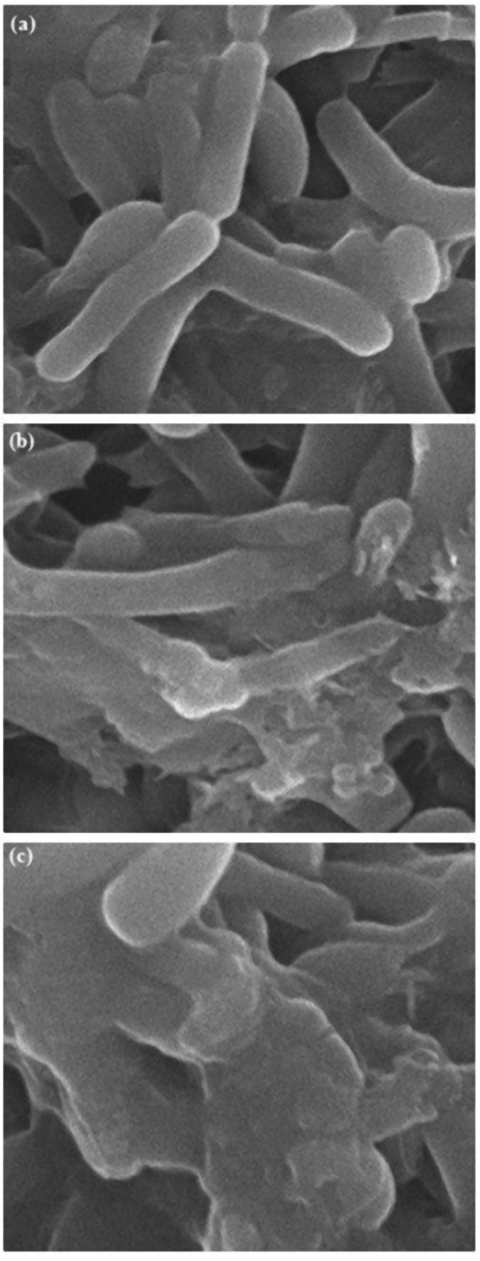

Figure 7: SEM micrographs of treated *Salmonella typhimurium* with phycosynthesized (*Sp*SeNPs-A) after 6 h (b) and 12 h (c), compared with control (a).

activity is dependent on the time of exposure of bacterial cells to *Sp*SeNPs. Therefore, this research work has further recognized that environment-friendly phycosynthesis of *Sp*SeNPs with enhanced phycochemical functionalities using *S. platensis* extract would be an economical and viable alternative to classical procedures.

Research funding: The authors state no funding involved.

Author contributions: Basant ElSaied: conceptualization, investigation, formal analysis, methodology, validation, writing – original draft, visualization; Amany Diab: investigation, methodology, supervision, validation, writing – review and editing; Ahmed Tayel: conceptualization, project administration, supervision, visualization, writing – review and editing; Mousa Alghuthaymi: data curation, funding acquisition, formal analysis, validation, resources; Shaaban Moussa: funding acquisition, data curation, formal analysis, validation, resources, writing – original draft.

Conflict of interest: The authors state no conflict of interest.

Data availability statement: All data generated or analyzed during this study are included in this published article. These datasets are also available from the corresponding author on reasonable request.

References

[1] Balabanian G, Rose M, Manning N, Landman D, Quale J. Effect of porins and bla_{KPC} expression on activity of imipenem with relebactam in Klebsiella pneumoniae: can antibiotic combinations overcome resistance? Microb Drug Resist. 2018;24(7):877–81. doi: 10.1089/mdr.2018.0065.

[2] Khan SA, Shahid S, Lee CS. Green synthesis of gold and silver nanoparticles using leaf extract of Clerodendrum inerme; characterization, antimicrobial, and antioxidant activities. Biomolecules. 2020;10(6):835. doi: 10.3390/biom10060835.

[3] Mendelson M, Matsoso MP. The World Health Organization global action plan for antimicrobial resistance. SAMJ. 2015;105(5):325. doi: 10.7196/SAMJ.9644.

[4] Li XZ, Nikaido H. Efflux-mediated drug resistance in bacteria. Drugs. 2009;69(12):1555–623. doi: 10.2165/11317030-000000000-00000.

[5] Centers for Disease Control and Prevention. Antibiotic resistance threats in the United States; 2019. Atlanta, GA. https://www.cdc.gov/drugresistance/pdf/threats-report/2019-ar-threats-report-508.pdf

[6] World Health Organization. New report calls for urgent action to avert antimicrobial resistance crisis. Joint News Release; 2019. p. 29. https://www.who.int/news-room/detail/29-04-2019-new-report-calls-for-urgent-action-to-avert-antimicrobial-resistancecrisis

[7] Khan SA, Lee CS. Green biological synthesis of nanoparticles and their biomedical applications. Applications of nanotechnology for green synthesis. Cham: Springer; 2020. p. 247–80. doi: 10.1007/978-3-030-44176-0_10.

[8] Ijaz F, Shahid S, Khan SA, Ahmad W, Zaman S. Green synthesis of copper oxide nanoparticles using Abutilon indicum leaf extract: antimicrobial, antioxidant and photocatalytic dye

degradation activitie. Trop J Pharm Res. 2017;16(4):743–53. doi: 10.4314/tjpr.v16i4.2.

[9] Khan SA, Shahid S, Shahid B, Fatima U, Abbasi SA. Green synthesis of MnO nanoparticles using abutilon indicum leaf extract for biological, photocatalytic, and adsorption activities. Biomolecules. 2020;10(5):785. doi: 10.3390/biom10050785.

[10] Shahid S, Fatima U, Sajjad R, Khan SA. Bioinspired nanotheranostic agent: zinc oxide; green synthesis and biomedical potential. Dig J Nanomater Biostruct. 2019;14:1023–31. doi: 10.3390/biom10050785.

[11] Khan SA, Noreen F, Kanwal S, Iqbal A, Hussain G. Green synthesis of ZnO and Cu-doped ZnO nanoparticles from leaf extracts of Abutilon indicum, Alerodendrum infortunatum, Clerodendrum inerme and investigation of their biological and photocatalytic activities. Mater Sci Eng. 2018;82:46–59. doi: 10.1016/j.msec.2017.08.071.

[12] Lateef A, Elegbede JA, Akinola PO, Ajayi VA. Biomedical applications of green synthesized-metallic nanoparticles: a review. Pan Afr J Life Sci. 2019;3:157–82. doi: 10.36108/pajols/9102/30(0170).

[13] Elegbede JA, Lateef A. Green synthesis of silver (Ag), gold (Au), and silver–gold (Ag–Au) alloy nanoparticles: a review on recent advances, trends, and biomedical applications. Nanotechnology and nanomaterial applications in food, health, and biomedical sciences. Palm Bay, FL: Apple Academic Press; 2019. p. 3–89. doi: 10.1201/9780429425660-1.

[14] Lateef A, Folarin BI, Oladejo SM, Akinola PO, Beukes LS, Gueguim-Kana EB. Characterization, antimicrobial, antioxidant, and anticoagulant activities of silver nanoparticles synthesized from Petiveria alliacea l. leaf extract. Prep Biochem Biotechnol. 2018;48(7):646–52. doi: 10.1080/10826068.2018.1479864.

[15] Xu C, Qiao L, Ma L, Yan S, Guo Y, Dou X, et al. Biosynthesis of polysaccharides-capped selenium nanoparticles using Lactococcus lactis NZ9000 and their antioxidant and anti-inflammatory activities. Front Microbiol. 2019;10:1632. doi: 10.3389/fmicb.2019.01632.

[16] Rayman MP. Selenium in cancer prevention: a review of the evidence and mechanism of action. Proc Nutr Soc. 2005;64(4):527–42. doi: 10.1079/PNS2005467.

[17] Gunti L, Dass RS, Kalagatur NK. Phytofabrication of selenium nanoparticles from Emblica officinalis fruit extract and exploring its biopotential applications: antioxidant, antimicrobial, and biocompatibility. Front Microbiol. 2019;10:931. doi: 10.3389/fmicb.2019.00931.

[18] Shirsat S, Kadam A, Naushad M, Mane RS. Selenium nanostructures: microbial synthesis and applications. RSC Adv. 2015;5(112):92799–811. doi: 10.1039/C5RA17921A.

[19] Shoeibi S, Mashreghi M. Biosynthesis of selenium nanoparticles using Enterococcus faecalis and evaluation of their antibacterial activities. J Trace Elem Med Biol. 2017;39:135–9. doi: 10.1016/j.jtemb.2016.09.003.

[20] Jalalian SH, Ramezani M, Abnous K, Taghdisi SM. Targeted co-delivery of epirubicin and NAS-24 aptamer to cancer cells using selenium nanoparticles for enhancing tumor response in vitro and in vivo. Cancer Lett. 2018;416:87–93. doi: 10.1016/j.canlet.2017.12.023.

[21] Zou J, Su S, Chen Z, Liang F, Zeng Y, Cen W, et al. Hyaluronic acid-modified selenium nanoparticles for enhancing the therapeutic efficacy of paclitaxel in lung cancer therapy. Artif Cell Nanomed Biotechnol. 2019;47(1):3456–64. doi: 10.1080/21691401.2019.1626863.

[22] Gahlawat G, Choudhury AR. A review on the biosynthesis of metal and metal salt nanoparticles by microbes. RSC Adv. 2019;9(23):12944–67. doi: 10.1039/C8RA10483B.

[23] Lee KX, Shameli K, Yew YP, Teow SY, Jahangirian H, Rafiee-Moghaddam R, et al. Recent developments in the facile bio-synthesis of gold nanoparticles (AuNPs) and their biomedical applications. Int J Nanomed. 2020;15:275. doi: 10.2147/IJN.S233789.

[24] Khanna P, Kaur A, Goyal D. Algae-based metallic nanoparticles: synthesis, characterization and applications. J Microbiol Methods. 2019;163:105656. doi: 10.1016/j.mimet.2019.105656.

[25] Asmathunisha N, Kathiresan K. A review on biosynthesis of nanoparticles by marine organisms. Colloids Surf B Biointerfaces. 2013;103:283–7. doi: 10.1016/j.colsurfb.2012.10.030.

[26] Muthusamy G, Thangasamy S, Raja M, Chinnappan S, Kandasamy S. Biosynthesis of silver nanoparticles from spirulina microalgae and its antibacterial activity. Env Sci Pollut Res. 2017;24(23):19459–64. doi: 10.1007/s11356-017-9772-0.

[27] Suganya KU, Govindaraju K, Kumar VG, Dhas TS, Karthick V, Singaravelu G, et al. Blue green alga mediated synthesis of gold nanoparticles and its antibacterial efficacy against Gram positive organisms. Mater Sci Eng. 2015;47:351–6. doi: 10.1016/j.msec.2014.11.043.

[28] Sayadi MH, Salmani N, Heidari A, Rezaei MR. Bio-synthesis of palladium nanoparticle using *Spirulina platensis* alga extract and its application as adsorbent. Surf Interfaces. 2018;10:136–43. doi: 10.1016/j.surfin.2018.01.002.

[29] Hifney AF, Abdel-Wahab DA. Phyco-based synthesis of TiO_2 nanoparticles and their influence on morphology, cyto-ultrastructure and metabolism of *Spirulina platensis*. Rend Lincei Sci Fis Nat. 2019;30(1):185–95. doi: 10.1007/s12210-019-00770-3.

[30] Xu C, Guo Y, Qiao L, Ma L, Cheng Y, Roman A. Biogenic synthesis of novel functionalized selenium nanoparticles by *Lactobacillus casei* ATCC 393 and its protective effects on intestinal barrier dysfunction caused by enterotoxigenic *Escherichia coli* K88. Front Microbiol. 2018;9:1129. doi: 10.3389/fmicb.2018.01129.

[31] Kokila K, Elavarasan N, Sujatha V. *Diospyros montana* leaf extract-mediated synthesis of selenium nanoparticles and their biological applications. N J Chem. 2017;41(15):7481–90. doi: 10.1039/C7NJ01124E.

[32] Gunasundari E, Kumar PS, Christopher FC, Arumugam T, Saravanan A. Green synthesis of metal nanoparticles loaded ultrasonic-assisted *Spirulina platensis* using algal extract and their antimicrobial activity. IET Nanobiotechnol. 2017;11(6):754–8. doi: 10.1049/iet-nbt.2016.0223.

[33] Elert EV, Jüttner F. Factors influencing the allelopathic activity of the planktonic cyanobacterium Trichormus doliolum. Phycologia. 1996;35(sup6):68–73. doi: 10.2216/i0031-8884-35-6S-68.1.

[34] Tayel AA, Moussa S, Opwis K, Knittel D, Schollmeyer E, Nickisch-Hartfiel A. Inhibition of microbial pathogens by

fungal chitosan. Int J Biol Macromol. 2010;47(1):10–4. doi: 10.1016/j.ijbiomac.2010.04.005.
[35] Marrie T, Costerton JW. Scanning and transmission electron microscopy of in situ bacterial colonization of intravenous and intraarterial catheters. J Clin Microbiol. 1984;19(5):687–93. doi: 10.1128/jcm.19.5.687-693.1984.
[36] Shubharani R, Mahesh M, Yogananda Murthy VN. Biosynthesis and characterization, antioxidant and antimicrobial activities of selenium nanoparticles from ethanol extract of bee propolis. J Nanomed Nanotechnol. 2019;10:1. doi: 10.4172/2157-7439.1000522.
[37] Faramarzi S, Anzabi Y, Jafarizadeh-Malmiri H. Nanobiotechnology approach in intracellular selenium nanoparticle synthesis using Saccharomyces cerevisiae – fabrication and characterization. Arch Microbiol. 2020;1–7. doi: 10.1007/s00203-020-01831-0.
[38] Michalak I, Chojnacka K. Algae as production systems of bioactive compounds. Eng Life Sci. 2015;15(2):160–76. doi: 10.1002/elsc.201400191.
[39] Liu HJ, Xu CH, Li WM, Wang F, Zhou Q, Li A, et al. Analysis of Spirulina powder by Fourier transform infrared spectroscopy and calculation of protein content. Spectrosc Spect Anal. 2013;33(4):977–81. doi: 10.3964/j.issn.1000-0593(2013)04-0977-05.
[40] Sheikhlou K, Allahyari S, Sabouri S, Najian Y, Jafarizadeh-Malmiri H. Walnut leaf extract-based green synthesis of selenium nanoparticles via microwave irradiation and their characteristics assessment. Open Agric. 2020;5(1):227–35.
[41] Phanjom P, Ahmed G. Effect of different physicochemical conditions on the synthesis of silver nanoparticles using fungal cell filtrate of *Aspergillus oryzae* (MTCC No. 1846) and their antibacterial effect. ANSN. 2017;8(4):045016. doi: 10.1088/2043-6254/aa92bc.
[42] Kumar R, Ghoshal G, Jain A, Goyal M. Rapid green synthesis of silver nanoparticles (AgNPs) using (*Prunus persica*) plants extract: exploring its antimicrobial and catalytic activities. J Nanomed Nanotechnol. 2017;8(4):1–8. doi: 10.4172/2157-7439.1000452.
[43] Dubey SP, Lahtinen M, Sillanpää M. Green synthesis and characterizations of silver and gold nanoparticles using leaf extract of Rosa rugosa. Colloids Surf A Physicochem Eng Asp. 2010;364(1–3):34–41. doi: 10.1016/j.colsurfa.2010.04.023.
[44] Vo TT, Nguyen TT, Huynh TT, Nguyen DT, Dang VS, Dang CH, et al. Biosynthesis of silver and gold nanoparticles using aqueous extract from *Crinum latifolium* leaf and their applications forward antibacterial effect and wastewater treatment. J Nanomater. 2019;2019:1–14. doi: 10.1155/2019/8385935.
[45] Huang F, Long Y, Liang Q, Purushotham B, Swamy MK, Duan Y. Safed *musli* (*Chlorophytum borivilianum L.*) *callus*-mediated biosynthesis of silver nanoparticles and evaluation of their antimicrobial activity and cytotoxicity against human colon cancer cells. J Nanomater. 2019;2019:2418785. doi: 10.1155/2019/2418785.
[46] Alvarez-Cirerol FJ, López-Torres MA, Rodríguez-León E, Rodríguez-Beas C, Martínez-Higuera A, Lara HH, et al. Silver nanoparticles synthesized with Rumex hymenosepalus: a strategy to combat early mortality syndrome (EMS) in a cultivated white shrimp. J Nanomater. 2019;2019:8214675. doi: 10.1155/2019/8214675.
[47] Nasrollahzadeh M, Sajadi SM. Pd nanoparticles synthesized in situ with the use of Euphorbia granulate leaf extract: catalytic properties of the resulting particles. J Colloid Interface Sci. 2016;462:243–51. doi: 10.1016/j.jcis.2015.09.065.
[48] Jummes B, Sganzerla WG, da Rosa CG, Noronha CM, Nunes MR, Bertoldi FC, et al. Antioxidant and antimicrobial poly-ε-caprolactone nanoparticles loaded with *Cymbopogon martinii* essential oil. Biocatal Agric Biotechnol. 2020;23:101499. doi: 10.1016/j.bcab.2020.101499.
[49] Fuller M, Köper I. Polyelectrolyte-coated gold nanoparticles: the effect of salt and polyelectrolyte concentration on colloidal stability. Polymers. 2018;10(12):1336. doi: 10.3390/polym10121336.
[50] Skoglund S, Hedberg J, Yunda E, Godymchuk A, Blomberg E, Odnevall Wallinder I. Difficulties and flaws in performing accurate determinations of zeta potentials of metal nanoparticles in complex solutions – four case studies. PLoS One. 2017;12(7):e0181735. doi: 10.1371/journal.pone.0181735.
[51] Sun Q, Cai X, Li J, Zheng M, Chen Z, Yu CP. Green synthesis of silver nanoparticles using tea leaf extract and evaluation of their stability and antibacterial activity. Colloids Surf A Physicochem Eng Asp. 2014;444:226–31. doi: 10.1016/j.colsurfa.2013.12.065.
[52] Ankamwar B, Damle C, Ahmad A, Sastry M. Biosynthesis of gold and silver nanoparticles using Emblica officinalis fruit extract, their phase transfer and transmetallation in an organic solution. J Nanosci Nanotechnol. 2005;5(10):1665–71.
[53] Zhang X, Yan H, Ma L, Zhang H, Ren DF. Preparation and characterization of selenium nanoparticles decorated by Spirulina platensis polysaccharide. J Food Biochem. 2020;44:e13363. doi: 10.1111/jfbc.13363.
[54] Oyaizu M. Studies on products of browning reaction. JSND. 1986;44(6):307–15. doi: 10.5264/eiyogakuzashi.44.307.
[55] Lee HJ, Song JY, Kim BS. Biological synthesis of copper nanoparticles using *Magnolia kobus* leaf extract and their antibacterial activity. J Chem Technol Biotechnol. 2013;88(11):1971–7. doi: 10.1002/jctb.4052.
[56] Park JC, Jeon GE, Kim CS, Seo JH. Effect of the size and shape of silver nanoparticles on bacterial growth and metabolism by monitoring optical density and fluorescence intensity. Biotechnol Bioproc E. 2017;22(2):210–7. doi: 10.1007/s12257-016-0641-3.
[57] Martínez-Castañon GA, Nino-Martinez N, Martinez-Gutierrez F, Martinez-Mendoza JR, Ruiz F. Synthesis and antibacterial activity of silver nanoparticles with different sizes. J Nanopart Res. 2008;10(8):1343–8. doi: 10.1007/s11051-008-9428-6.
[58] Menon S, Agarwal H, Rajeshkumar S, Rosy PJ, Shanmugam VK. Investigating the antimicrobial activities of the biosynthesized selenium nanoparticles and its statistical analysis. BioNanoScience. 2020;10:1–4. doi: 10.1007/s12668-019-00710-3.
[59] Vyas J. Green synthesis of selenium nanoparticles using allium sativum extract. Asian J Biol Life Sci. 2017;6(3):436–40. doi: 10.21276/ijpbs.2019.9.1.46.
[60] Fardsadegh B, Jafarizadeh-Malmiri H. Aloe vera leaf extract mediated green synthesis of selenium nanoparticles and assessment of their in vitro antimicrobial activity against spoilage fungi and pathogenic bacteria strains. Green Process Synth. 2019;8(1):399–407. doi: 10.1515/gps-2019-0007.

[61] Vasić S, Radojević I, Pešić N, Čomić L. Influence of sodium selenite on the growth of selected bacteria species and their sensitivity to antibiotics. Kragujev J Sci. 2011;33:55–61.
[62] Man NY, Knight DR, Stewart SG, McKinley AJ, Riley TV, Hammer KA. Spectrum of antibacterial activity and mode of action of a novel tris-stilbene bacteriostatic compound. Sci Rep. 2018;8(1):1–9. doi: 10.1038/s41598-018-25080-w.
[63] Dong Y, Zhu H, Shen Y, Zhang W, Zhang L. Antibacterial activity of silver nanoparticles of different particle size against *Vibrio natriegens*. PLoS One. 2019;14(9):e0222322. doi: 10.1371/journal.pone.0222322.
[64] Khiralla GM, El-Deeb BA. Antimicrobial and antibiofilm effects of selenium nanoparticles on some foodborne pathogens. LWT. 2015;63(2):1001–7. doi: 10.1016/j.lwt.2015.03.086.
[65] Mulla NA, Otari SV, Bohara RA, Yadav HM, Pawar SH. Rapid and size-controlled biosynthesis of cytocompatible selenium nanoparticles by *Azadirachta indica* leaves extract for anti-bacterial activity. Mater Lett. 2020;264:127353. doi: 10.1016/j.matlet.2020.127353.
[66] Geoffrion LD, Hesabizadeh T, Medina-Cruz D, Kusper M, Taylor P, Vernet-Crua A, et al. Naked selenium nanoparticles for antibacterial and anticancer treatments. ACS Omega. 2020;5(6):2660–9. doi: 10.1021/acsomega.9b03172.
[67] Fardsadegh B, Vaghari H, Mohammad-Jafari R, Najian Y, Jafarizadeh-Malmiri H. Biosynthesis, characterization and antimicrobial activities assessment of fabricated selenium nanoparticles using *Pelargonium zonale* leaf extract. Green Process Synth. 2019;8(1):191–8. doi: 10.1515/gps-2018-0060.
[68] Al-Saggaf MS, Tayel AA, Ghobashy MOI, Alotaibi MA, Alghuthaymi MA, Moussa SH. Phytosynthesis of selenium nanoparticles using costus extract for bactericidal application against foodborne pathogens. Green Process Synth. 2020;9:477–87. doi: 10.1515/gps-2020-0038.